CHINA FOUNDRY Research & Development
Vol.13 No.1 January 2016
DOI: 10.1007/s41230-016-5014-1

Microstructure and elevated-temperature tensile properties of differential pressure sand cast Mg-4Y-3Nd-0.5Zr alloy

Hong-hui Liu [1,2], *Zhi-liang Ning [1,3], Hai-chao Sun [1,3], Fu-yang Cao [1,3], Hao Wang [1,3], Xin-yi Zhao, and Jian-fei Sun [1,3]

1. School of Materials Science and Engineering, Harbin Institute of Technology, Harbin 150001, China;

2. Harbin Dongan Engine (Group) Co. Ltd., Harbin 150066, China;

3. National Key Laboratory for Precision Hot Processing of Metals, Harbin Institute of Technology, Harbin 150001, China

Abstract: The microstructures of an Mg-4Y-3Nd-0.5Zr alloy by differential pressure casting were investigated using scanning electron microscopy (SEM) and transmission electron microscopy (TEM), and its tensile deformation behavior was measured using a Gleeble1500D themo-simulation machine in the temperature range of 200 to 400 °C at initial strain rates of 5×10^{-4} to 10^{-1} s^{-1}. Results show that the as-cast microstructure consists of primary α-Mg phase and bone-shaped Mg_5RE eutectic phase distributed along the grain boundary. The eutectic phase is dissolved into the matrix after solution treatment and subsequently precipitates during peak aging. Tensile deformation tests show that the strain rate has little effect on stress under 300 °C. Tensile stress decreases with an increase in temperature and the higher strain rate leads to an increase in stress above 300 °C. The fracture mechanism exhibits a mixed quasi-cleavage fracture at 200 °C, while the fracture above 300 °C is a ductile fracture. The dimples are melted at 400 °C with the lowest strain rate of 10^{-4} s^{-1}.

Key words: Mg-4Y-3Nd-0.5Zr alloy; microstructure; mechanical property at elevated temperature; fracture

CLC numbers: TG146.22 **Document code:** A **Article ID:** 1672-6421(2016)01-030-06

Magnesium alloys are considered potential candidates for many structure applications due to low density, excellent castability and machinability [1-4]. Mg-RE-Zr alloys, as a group of special light alloys, have important applications in aerospace, military, automotive, and other industries [5-7]. The most successful magnesium alloys developed to date have been those based on the Mg-Y-Nd system, identified as WE43 (4wt.%Y-3wt.%RE-0.5wt.%Zr) and WE54 (5wt.%Y-4wt.%RE-0.5wt.%Zr) by Magnesium Elektron Company, England. The strengths of these alloys are achieved essentially via precipitation strengthening. The microstructural evolution and mechanical properties of these commercial alloys have been well documented in general [8-11]. They are adequate for long-term service at temperatures up to 250 °C under stressed conditions. In general, WE alloys are cast under gravity. In this study, a WE43 alloy with normal compositions of Mg-4Y-3Nd-0.5Zr without containing other heavy rare earth elements was cast by differential pressure and gravity. Its microstructure and tensile deformation behavior at elevated temperature were also investigated.

***Zhi-liang Ning**

Male, born in 1966, Ph.D, Associate Professor. His research interests mainly focus on nonferrous alloys and their applications.

E-mail: zhiliangning@sina.com

Received: 2015-03-16; Accepted: 2015-12-01

1 Experimental procedure

The Mg-4Y-3Nd-0.5Zr alloy was melted in a mild steel crucible using an electrical resistance furnace. The starting materials were 99.9%Mg, 99.9%Y, Mg-30%Nd master alloy and Mg-33.3%Zr master alloy. The mixture was protected by RJ2 cover flux [main compositions: 38%–46% $MgCl_2$, 32%–40% KCl, 5%–8% $BaCl_2$, 3%–5% CaF_2, and 8% (NaCl+CaCl)]. The magnesium ingot was melted in the steel crucible first, and then pure Y and Mg-Nd were added at 720 °C and Mg-Zr master alloy was added at 750 °C. After stirring, the melt was held at 780 °C for 30 min to ensure all alloy elements were completely dissolved. RJ5 flux [main compositions: 24%–30% $MgCl_2$, 20%–26% KCl, 28%–31% $BaCl_2$,13%–15% CaF_2, and 8% (NaCl+CaCl)]

was used as refining agent. Following this procedure, the melt was cast into a sand mould by differential pressure at 730 °C. Raising speed at pressurizing stage and holding pressure were 1 KPa•s^{-1} and 40 KPa, respectively.

The chemical composition was Mg-3.78%Y-3.2%Nd-0.43%Zr (in wt.%) that were measured by an Inductively Coupled Plasma-Atomic Emission Spectroscopy (ICP-AES). The phases of as-cast sample were determined by D/max-rB X-ray diffractometer (XRD). All samples for microstructural observation and specimens for mechanical tests at elevated temperatures were cut from the casting at the position with the maximum thickness of 38 mm. In addition, 24 samples were taken from the desired positions at both gravity and differential pressure castings for a comparison of the mechanical properties at the room temperature. For the heat treatment, the specimens were firstly solution treated at 525±5 °C for 8 h, followed by quenching in water of 50 °C and finally artificially peak aged at 250±5 °C for 16 h. Small metallographic samples cut from both as-cast and heat treated castings were mounted in cold-setting epoxy resin for microstructural observation. All samples were ground initially with SiC paper down to 1200 grit grade, followed by polishing with 6 μm and 1 μm diamond suspensions. The samples were etched by 4% HNO_3. The grain structures of the samples were examined and photographed using an optical microscope (Olympus BH-2). Both as-cast and solution heated microstructures were analyzed using a FEI Sirion scanning electron microscope (SEM) operated at 20 kV and transmission electron microscopy (TEM, Tecnai G2 F30) operated at 120 kV, respectively.

Tensile specimens with a gauge section of 1.6 mm × 5 mm were cut from the heat treated castings. The tensile test at elevated temperature was carried out on a Gleeble-1500D Instron electronic universal materials testing machine with initial strain rates ranging from 5×10^{-4} to 1×10^{-1} s^{-1} at temperatures up to 400 °C. Prior to testing, the samples were heated at a speed of 1 K•s^{-1} from room temperature to the selected temperature, followed by a holding period of 300 s to maintain temperature uniformity. The test chamber was protected with Ar gas to avoid the oxidation. And then, the fractured morphologies of samples were examined by SEM.

2 Results

2.1 Microstructure

The microstructure of as-cast Mg-4Y-3Nd-0.5Zr alloy consists of primary α-Mg and Mg_5RE phases, which is shown in the XRD curve in Fig. 1. The microstructure under OM and SEM are shown in Fig. 2(a-c). Due to the addition of Zr, the average grain size of as-cast alloy is around 78 μm, even the sample was cut from the relatively thick wall of 38 mm with a low cooling rate. The eutectic Mg-RE phase distributes at the grain boundary, as shown in Fig. 2(a). Figure 2(b) shows the enlarged eutectic phase with the bone-shaped morphology marked with a red arrow. As shown in Fig. 2(c), the element of eutectic phase is approximately $Mg_5(Nd_{0.64}Y_{0.36})$ measured by EDS, which is in good agreement with Apps' study [10].

After solution treatment, the $Mg_5(Nd_{0.64}Y_{0.36})$ phase at the grain boundary is completely in solution into the matrix and subsequently precipitates during peak aging. However, the Y-enriched cuboid-shaped phase still remains in the matrix due to thermal stability. The as-cast

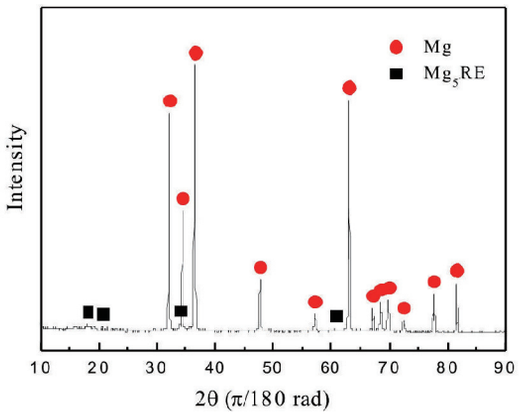

Fig. 1: XRD of as-cast Mg-3Y-4Nd-0.5Zr alloy

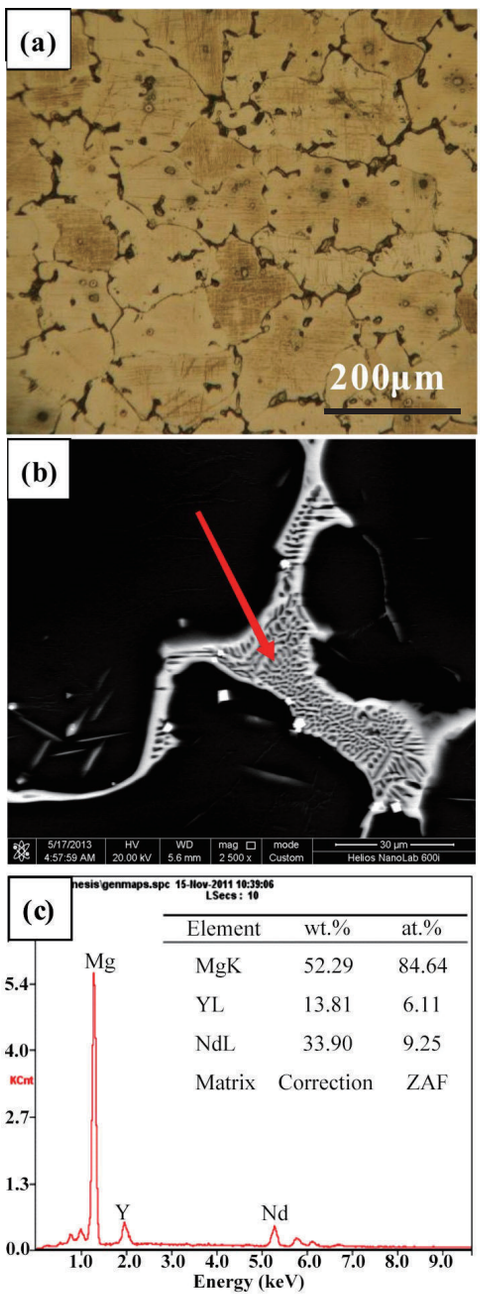

Fig. 2: As-cast microstructures of Mg-3Y-4Y-0.5Zr alloy: (a) optical microstructure, (b) enlarged eutectic phase in SEM, and (c) EDS of bone-shaped phase showed in Fig. 2(b)

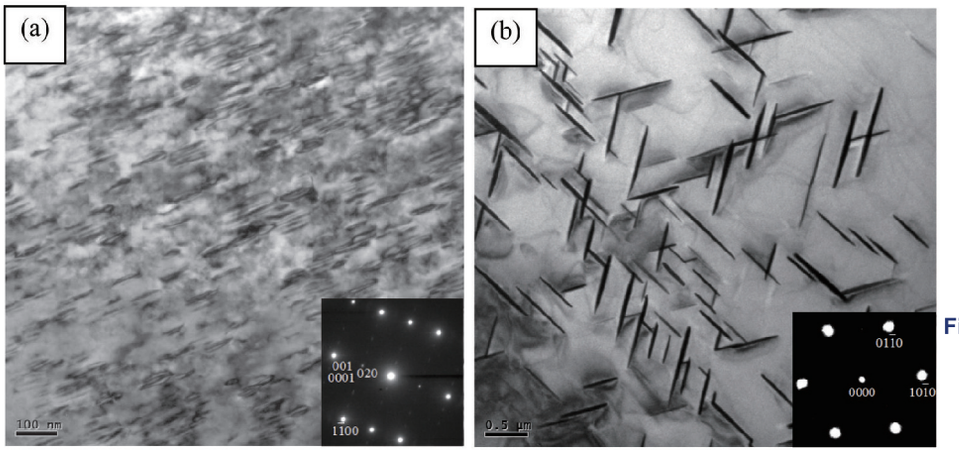

Fig. 3: TEM and SAED patterns for precipitates at [1120] (a) and [0001] (b)

grains change from irregular to hexagonal, and the average grain size is increased to 88 μm with a relatively large error after heat treatment. After peak aging, some disk-like phases with face-center cubic structures, as shown in Fig. 3, are precipitated from the matrix. The precipitated phase mainly consists of β' when aged at 250 °C for 16 h [8].

2.2 Tensile properties

The typical engineering stress-strain curves at different conditions are shown in Fig. 4 (a-e). It can be seen that the strain rate has little effect on engineering stress under 300 °C, while the engineering stress increases sharply with increased engineering strain to reach a peak, followed by a relatively slow increase until fracture. However, at 350 °C, the engineering stress quickly reaches a peak, followed by a slight increase until fracture at higher strain rate. In addition, it can be found that the engineering strain reaches a peak

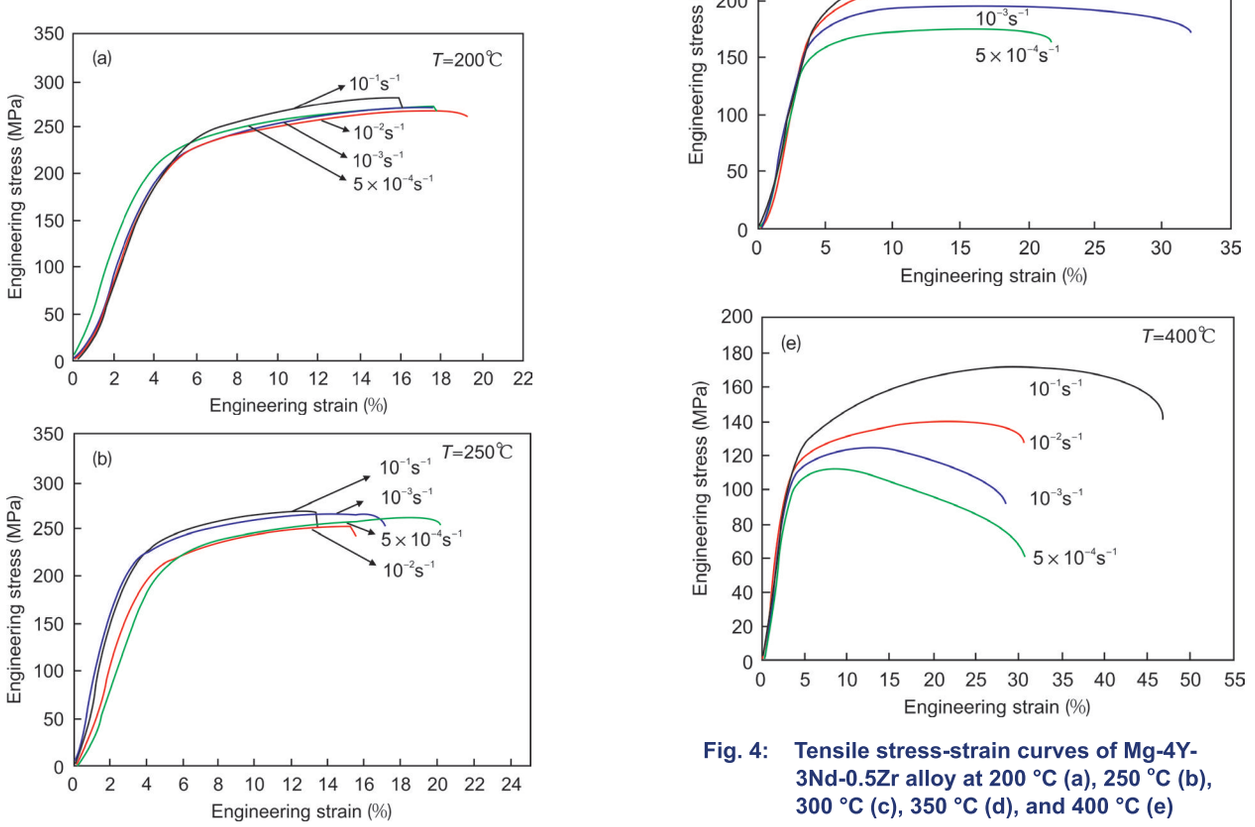

Fig. 4: Tensile stress-strain curves of Mg-4Y-3Nd-0.5Zr alloy at 200 °C (a), 250 °C (b), 300 °C (c), 350 °C (d), and 400 °C (e)

and remains constant before fracture at a lower strain rate with the temperature range of 300-350 °C. When the temperature is increased to 400 °C, the strain rate has a significant effect on engineering stress, and it has an obvious decrease before fracture, especially at a lower strain rate. The ultimate strengths against test temperature are shown in Table 1 and it is worth noting that the ultimate strengths of the alloy are higher than the standards of Elektron WE43 alloy [12].

2.3 Fracture analysis

The fractured surfaces of tested specimens at different temperatures are given in Fig. 5. The alloy reveals a mixed fracture with small tearing ridges, cleavage facets and dimples which become deeper with decreased strain rate at 200 °C, as shown in Fig. 5(a) and (b). When deformation temperature increases to 300 °C, the cleavage plane disappears partially, some cuboid-shaped Mg-RE phase and secondary crack are observed, as shown in Fig. 5(c). With the increasing of temperature to 400 °C, the fractography shows a typical ductile rupture with deeper dimple, as given in Fig. 5 (d). There is an oxidation film on the fracture surface when tested at a lower strain rate due to the long deformation time at a higher deformation temperature, as shown in Fig. 5 (e). It is well known that magnesium has a hexagonal close-packed (h.c.p) crystal structure with limited slip systems.

Table 1: Ultimate tensile stress measured at various temperatures and strain rates (MPa)

Temp.	Strain rate, s^{-1}				
	$1x10^{-1}$	$1x10^{-2}$	$1x10^{-3}$	$5x10^{-4}$	Ref. [12]
200 °C	281	264	266	265	258
250 °C	266	255	263	262	232
300 °C	243	246	249	241	175
350 °C	224	216	190	171	
400 °C	168	134	120	110	

* The strain rate for the ultimate stresses measured in Ref. [12] were not given.

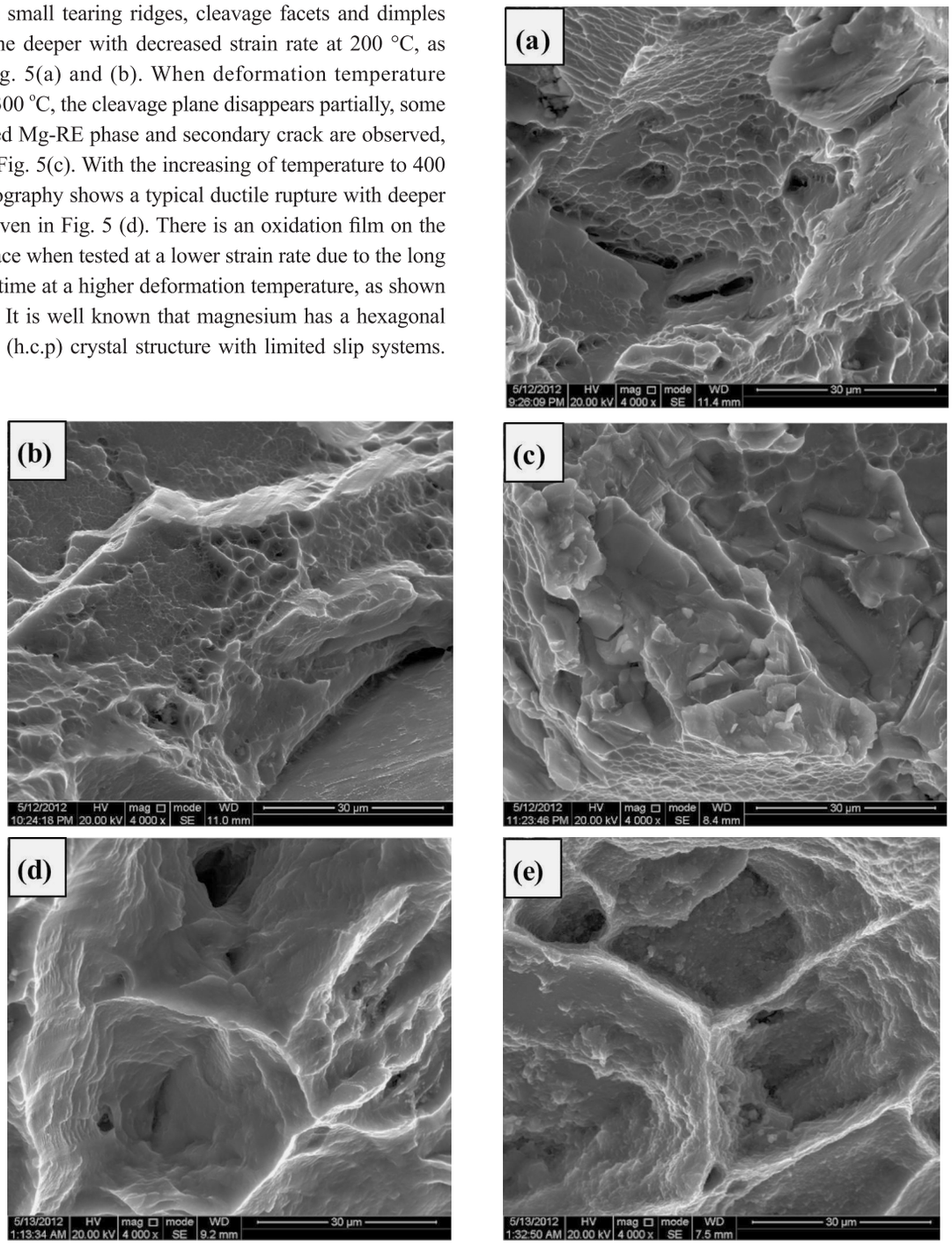

Fig. 5: Tensile fractographies of Mg-4Y-3Nd-0.5Zr alloy tested at 200 °C, ε=10^{-1} s^{-1} (a), 200 °C, ε=10^{-3} s^{-1} (b), 300 °C, ε=10^{-1} s^{-1} (c), 400 °C, ε=10^{-1} s^{-1} (d), and 400 °C, ε=5×10^{-4} s^{-1} (e)

The main deformation mechanisms of h.c.p crystal structure are the basal slip, the prismatic slip, the pyramidal slip and twinning. The main slip system of the h.c.p at room temperature is the (0001) basal plane, which is 100 times easier compared to the other non-basal plane slip systems [13]. At elevated temperatures, plastic deformation of magnesium begins with activation of the soft basal slip system, followed by prismatic and other hard slip systems as the internal stresses increase, resulting in a significantly increased elongation to fracture.

3 Discussion

According to the phase diagrams, the solubility of Y and Nd in Mg can reach 12.4wt.% and 3.6wt.% at 567 °C and 552 °C, respectively, and decrease gradually with decreased temperature through to room temperature [14, 15]. The solid solubility of all REs in Mg is negligible below 200 °C. The chemical composition of the alloy investigated is Mg-3.78%Y-3.2%Nd-0.43%Zr, while Zr acts as a refiner. Under non-equilibrium solidification condition, the Mg-RE compounds form finally at the grain boundaries. The Mg-RE phase with bright contrast within the eutectic phase implies that Mg-RE particles act as nucleus of the eutectic phase during solidification [16]. During solution treatment, the $Mg_5(Nd_{0.64}Y_{0.36})$ phase at the grain boundary is completely dissolved into the matrix and the morphology of grain becomes hexagonal, with a slight increase in grain size due to some small grains amalgamating.

During aging, the Mg-RE compounds precipitate from the supersaturated matrix. The precipitated sequence in Mg-Y-Nd alloys was well investigated to be involved the formation of β', β" and β phase particles depending upon aging temperature [8,9,11]. The metastable phase β' has a D019 crystal structure (hexagonal, a=0.642 nm, c=0.521 nm). The intermediate phase β" has a base-centered orthorhombic structure (a=0.640 nm, b=2.223 nm, c=0.521 nm), and the equilibrium phase β is face-centered cubic (a=2.223 nm). At peak aging at 250 °C, the precipitate mainly consists of β' phase [8].

The solubility of RE is decreased by multi-rare element additions, resulting in an enhanced amount of precipitates. The strength of Mg-RE alloys is increased by means of inhibiting the movement of grain boundaries and pinning up dislocations by precipitates [6]. On the other hand, the mechanical properties of a casting are closely related to the internal defects. For the purposes of this study, the casting was produced by differential pressure casting with a pressure of 40 kPa during solidification. Therefore, the amount of defects, such as shrinkage and gas pores, was reduced or eliminated completely, which is expected to generally improve the mechanical properties by decreasing the number of voids and micro-cracks.

The measured mechanical properties at room temperature are shown in Table 2. The investigation of the mechanical properties of this alloy by both gravity casting and differential pressure casting, of which 24 samples were taken from the same positions, shows that the ultimate tensile strength is increased by 8.8%–14.7% and the elongation to fracture is increased by 155%–186%, which indicates that the mechanical properties of Mg alloy casting could be effectively improved through the differential pressure casting.

Table 2: Mechanical properties of castings by gravity cast and differential pressure cast

Positions	Gravity casting		Differential pressure casting	
	UTS (MPa)	El (%)	UTS (MPa)	El (%)
1	243	2.5	278	6.5
2	264	3.5	293	10.0
3	258	3.5	293	9.5
4	261	3.0	287	8.5
5	248	3.5	275	9.0
6	267	2.5	290	7.0
7	245	4.0	272	11.0
8	274	3.5	294	10.0
9	250	4.5	273	11.5
10	252	2.5	288	7.0
11	242	2.5	279	6.5
12	257	4.0	286	10.5
13	260	3.5	290	10.0
14	235	2.0	268	5.5
15	262	3.0	292	8.0
16	238	2.0	273	5.5
17	261	3.0	288	8.5
18	272	3.5	296	9.5
19	248	2.5	284	6.5
20	254	2.0	280	5.5
21	265	4.0	292	11.0
22	261	3.0	288	8.5
23	248	2.5	270	6.5
24	259	3.0	284	8.5

4 Conclusions

(1) The microstructures of an Mg-4Y-3Nd-0.5Zr alloy by differential pressure casting consist of primary α-Mg phase and bone-shaped Mg_5RE eutectic phase distributed along the grain boundaries. The eutectic phase is dissolved into the matrix after solution treatment and subsequently precipitates during the aging process which strengthens the alloy.

(2) The strain rate has little effect on engineering stress when the temperature is below 300 °C. Tensile stress decreases with the increase of temperature. When the temperature is above 300 °C, tensile stress is obviously higher at a high strain rate than at a low strain rate, which are different with temperatures under 300 °C.

References

[1] Fu P H, Peng L M, Jiang H Y, et al. Tensile properties of high strength cast Mg alloys at room temperature: A review. China Foundry, 2014, 11(4): 277–286.
[2] Tao J Q, Wan Y Y, Sun C J, et al. Microstructure evolution of an Mg-Zn-Nd-Zr magnesium alloy during recrystallization and partial remelting process. China Foundry, 2013, 10(4): 244–247.
[3] Li Q A, Zhang Q, Wang Y G, et al. Effects of Sm addition on microstructure and mechanical properties of a Mg-10Y alloy. China Foundry, 2014, 11(1): 28–32.
[4] Golmakanniyoon S, Mahmudi R. Microstructure and creep behavior of the rare-earth doped Mg-6Zn-3Cu cast alloy. Mater. Sci. Eng., A, 2011, 528: 1668–1677.
[5] Ning Z L, Liu H H, Cao F Y, et al. The effect of grain size on the tensile and creep properties of Mg-2.6Nd-0.35Zn-xZr alloys at 250 ºC. Mater. Sci. Eng., A, 2013, 560: 163–169.
[6] Ning Z L, Wang H, Liu H H, et al. Effects of Nd on microstructures and properties at the elevated temperature of a Mg-0.3Zn-0.32Zr alloy. Mater. Des., 2010, 31(9): 4438–4444.
[7] Janik V, Yin D D, Wang Q D, et al. The elevated-temperature mechanical behavior of peak-aged Mg-10Gd-3Y-0.4Zr alloy. Mater. Sci. Eng., A, 2011, 528(7–8): 3105–3112.
[8] Mengucci P, Barucca G, Riontino G, et al. Structure evolution of a WE43 Mg alloy submitted to different thermal treatments. Mater. Sci. Eng., A 479, 2008:37–44
[9] Barucca G, Ferragut R, Fiori F, et al. Formation and evolution of the hardening precipitates in a Mg-Y-Nd alloy. Acta Mater., 2011, 59: 4151–4158.
[10] Apps P J, Karimzadeh H, King J K, et al. Phase compositions in magnesium-rare earth alloys containing yttrium, gadolinium or dysprosium. Scripta Mater., 2003, 48: 475–481.
[11] Xin R L, Li L, Zeng K, et al. Structural examination of aging precipitation in a Mg-Y-Nd alloy at different temperatures. Mater. Charact., 2011, 62: 535–539.
[12] http://www.magnesium-elektron.com/site-map.asp Magnesium Elektron Service & Innovation in Magnesium. Elektron WE43. Datasheet: 467, Accessed 06 January 2014.
[13] Zainuddin B S, Yukio M, Yasunobu H, et al. Effects of Mn content and texture on fatigue properties of as-cast and extruded AZ61 magnesium alloys. Int. J. Mech. Sci., 2006, 48(2): 198–209.
[14] Zhao H D, Qin G W, Ren Y P, et al. The maximum solubility of Y in α-Mg and composition ranges of $Mg_{24}Y_{5-x}$ and Mg_2Y_{1-x} intermetallic phases in Mg-Y binary system. J. Alloys Compd., 2011, 509(3): 627–631.
[15] Chia T L, Easton M A, Zhu S M, et al. The effect of alloy composition on the microstructure and tensile properties of binary Mg-rare earth alloys. Intermet., 2009, 17: 481–490.
[16] Golmkaniyoon S and Mahmudi R. Comparison of the effects of La-and Ce-rich rare earth additions on the microstructure, creep resistance, and high-temperature mechanical properties of Mg-6Zn-3Cu cast alloy. Mater. Sci. Eng., A, 2011, 528(15): 5228–5233.

This work was supported by the Ministry of Science and Technology of China through Grant 2009GJB 2001.1